Calculated and Measured Line Intensity Ratios of Singly and Doubly Ionized Nitrogen Atoms in a Hydrogen Plasma

by

John Douglas Hey

Thesis presented in partial fulfilment of the requirements for the degree of M.Sc. in Physics at the University of Cape Town

May, 1970

Index

Abstract

The oscillator strengths of several NII and NIII lines in the optical wavelength region are calculated by means of the Coulomb approximation. Atomic processes in a plasma are discussed, as well as two models (LTE and semi-coronal) which can be used to determine the line intensity ratios of subsequent ionization stages of the same element. Two derivations of line intensity ratio formulae are given, valid under LTE and semi-coronal conditions. Parameters necessary for the evaluation of collisional-radiative coefficients in the semi-coronal model are discussed, and an attempt is made to show that the theoretical values in the literature at present, are inadequate under the laboratory conditions of interest. The lines for which f-values have been calculated are generated in a theta pinch plasma, and an attempt is made to decide which of the two models accounts more accurately for the observed intensity ratios.

Introduction

In this thesis an attempt is made to establish the form of the equations determining the line intensity ratios of subsequent ionization stages of the same element, valid under semi-coronal conditions (electron temperatures between 1 and 10 eV and densities of the order of 10^{15} to 10^{16} per cm^3).

An important parameter in plasma spectroscopy is the absorption oscillator strength, f, of a transition. The first chapter is devoted to a discussion of a relatively simple atomic model, the Coulomb approximation, which leads to satisfactory values of f in most cases of interest.

Inside a plasma, the state of the atoms could range from neutral to highly ionized. Under conditions of local thermal equilibrium (LTE), the ratio of the population densities of excited levels within an atom or ion, and of successive ionization stages, are determined by the Boltzmann and Saha equations. Line intensity ratios can then readily be determined using oscillator strengths evaluated by means of the Coulomb approximation. In the second chapter, atomic processes are discussed and it is

shown that in our case neither complete LTE nor coronal equilibrium can be expected to describe the thermodynamic situation accurately and that certain semi-coronal coefficients need to be determined before semi-coronal line intensity ratios can be calculated.

There is much uncertainty in the literature about the values of these collisional-radiative coefficients (Chapter 3) under semi-coronal conditions, particularly for non-hydrogenic atoms. An attempt is made to decide whether with the large uncertainties that the semi-coronal approach involves, the LTE formulae do not lead to line intensity ratios in better agreement with the corresponding measured quantities.

The last two chapters are devoted to experimental considerations and results.

Chapter 1 : Oscillator Strengths

The type of plasma used in this project is classed as "optically thin", i.e. very little emitted radiation is re-absorbed by the plasma, and photon densities are low. The exceptions to this rule are the resonance lines (longest wavelengths capable of exciting fluorescence) of the various atomic species, which are fairly strongly re-absorbed. However, for reasons outlined in the section on "Atomic Processes", these do not concern us here. Denoting by A_{pm} the Einstein coefficient for a spontaneous transition by the radiating atom or ion from state m to state p with emission of a photon, the line intensity for this transition may be written:

$$I = N_m^z A_{pm} h\nu_{pm} \qquad (1.1)$$

Here N_m^z is the number of ions of a particular species, charge z, in state m.

A dimensionless quantity which is used extensively in spectroscopy is the oscillator strength or f-value of a transition. Originally introduced from classical theory, the absorption oscillator strength f_{mp} is defined in terms of A_{pm} by

$$A_{pm} = \frac{2r_o\omega_{pm}^2 g_p f_{mp}}{c\, g_m} \qquad (1.2)$$

where r_o is the classical electron radius. From equation (1.1) it follows that the line intensity is known provided the f-value of the transition, as well as the number of atoms in state m, are known.

Related to f is the line strength S of the transition:

$$f_{mp} = \frac{8\pi^2\, m\, c}{3he^2 g_p \lambda} S_{mp} = \frac{303.75}{g_p \lambda} S_{mp} \qquad (1.3)$$

where λ is in $\mathring{A}$, and g_p is the statistical weight of the lower state involved in the transition. Here S_{mp} is expressed in atomic units, which are, for (allowed) electric dipole transitions:

$$a_o^2 e^2 = 6.459 \times 10^{-36}\ \text{cm}^2\ \text{esu}^2$$

It is customary to write S_{mp} in terms of the relative line strength S(L) and relative multiplet strength S(M) (see equation (1.7) below). Let ℓ' and ℓ'' denote the initial and final orbital quantum numbers of the "jumping" electron, and denote the greater of the two by $\ell_>$. The symbols S, L, J represent the spin, orbital and total

angular momentum quantum numbers of the initial state; similarly S', L', J' those of the final state. The "core" (parent) is designated by its orbital angular momentum L_1, which is assumed not to change during the transition. To avoid confusion, the initial state is taken to be the state of lower energy measured from the ground state of the species.

S(L) and S(M) are expressed in terms of so-called Racah coefficients. Values of the two types of Racah coefficients which are needed to evaluate S_{mp}, viz. W(LJL'J'; S 1) and W(ℓ'Lℓ"L'; L_1 1) are listed in Griem's "Plasma Spectroscopy"(1). One then has:

$$S(L) = \frac{(2J+1)(2J'+1)W^2(LJL'J';S\ 1)}{(2S+1)} \qquad (1.4)$$

$$S(M) = (2S+1)(2L+1)(2L'+1)\ell_>(4\ell_>^2-1)W^2(\ell'L\ell"L';\ L_1\ 1) \qquad (1.5)$$

In accordance with the selection rules, it is assumed that S = S'.

Values of S(L) and S(M) calculated using the Racah coefficients may be checked by comparing them with the earlier (incomplete) tabulations of Russell (2) and

Goldberg (3),(4). Allen (5) reprints Russell's and Goldberg's tables, and incorporates the correction factors listed in (4).

The atomic model used in this thesis for calculating oscillator strengths is the Coulomb approximation, which is described in the following paragraphs. Russell-Saunders coupling is assumed and all quantities are expressed in atomic units.

Let $\frac{R_i}{r}$ and $\frac{R_f}{r}$ be the initial and final radial wave functions of the active electron normalized in atomic units. From the Schrödinger equation, R_i and R_f satisfy:

$$\frac{d^2R}{dr^2} + \left(2v - \frac{\ell(\ell+1)}{r^2} - \varepsilon\right)R = 0 \qquad (1.6)$$

where v is the potential, ℓ the azimuthal quantum number and ε the energy parameter. One method of solution would be to integrate numerically outward from the origin, ε being adjusted to be an eigenvalue; a disadvantage of this approach is that an exact knowledge of v is required.

However, if it is assumed that v approximates closely to its asymptotic form before the region is reached which gives the dominant contribution to the transition integral

$$\int_0^\infty R_i R_f \, r dr \quad ,$$

v may be replaced by $^{C}/_{r}$, C being the excess charge on the nucleus when the active electron is removed. D.R. Bates and A. Damgaard (6) have justified this assumption in the case of many transitions of interest, and show that it readily leads to a solution of equation (1.6).

Then, S_{mp} is given by

$$S_{mp} = S(M)S(L)\sigma^2 \tag{1.7}$$

where

$$\sigma^2 = \frac{1}{(4\ell_>^2 - 1)} \left(\int_o^\infty R_i R_f \, rdr \right)^2 \tag{1.8}$$

Screening is taken into account by the introduction of the effective principal quantum number $n^* = \frac{C}{\sqrt{\epsilon}}$ and for reasons of presentation, σ is expressed as

$$\sigma(n^*_{\ell-1}, \ell-1; n^*_\ell, \ell; C) = \frac{1}{C} \mathcal{F}(n^*, \ell) \mathcal{G}(n^*_{\ell-1}, n^*_\ell, \ell) \tag{1.9}$$

where $\mathcal{F}(n^*_\ell, \ell) = \left[\frac{3n^*_\ell}{2} \left\{ \frac{(n^{*2}_\ell - \ell^2)}{(4\ell^2 - 1)} \right\}^{\frac{1}{2}} \right]$

and

$$\mathcal{G}(n^*_{\ell-1}, n^*_\ell, \ell) = \left[\frac{2C}{3n^*_\ell (n^{*2}_\ell - \ell^2)^{\frac{1}{2}}} \right] \int_o^\infty R(n^*_{\ell-1}, \ell-1, C) R(n^*_\ell, \ell, C) \times rdr$$

Referring to the notation used in connection with the Racah coefficients (equation 1.5),

$$\ell' = \ell - 1 \qquad \ell'' = \ell$$

the lower ℓ value pertaining to the state of lower energy with respect to the ground state in the transitions studied here (with two exceptions - see f tables).

In the paper of Bates and Damgaard, numerical values of $\mathcal{F}$ and $\mathcal{G}$ are tabulated for $\ell = 1$ (s-p transitions), $\ell = 2$ (p-d transitions) and $\ell = 3$ (d-f transitions). This method, besides having the advantage of allowing f-values to be calculated reasonably quickly, gives accurate results for atoms with a single electron outside a closed shell; it is less accurate but still satisfactory when there are two or more outer electrons. The tables as compiled are most useful for s-p transitions; it has been found that a few p-d and d-f transitions fall outside the range of the $\mathcal{F}$ and $\mathcal{G}$ values given.

In most cases listed in this thesis, the f values have been calculated by the present writer, and, where possible, the results have been compared with those listed in (1) and "Atomic Transition Probabilities", a data compilation by Wiese, Smith and Glennon (7). As regards the reliability of the above approach compared with more

sophisticated methods, it may be of interest to quote from the introduction to (7) :

"On the whole the Coulomb approximation has given impressive results and has proved to be of great value. In most cases where comparisons are available - there are several hundred of them for the first ten elements - the results agree within 20 - 40 percent with those from advanced theoretical and experimental methods. We have therefore made extensive use of this approximation to supplement the available material".

In this thesis, some use has been made of the older term value tabulations of Bacher and Goudsmit (8) besides those in (7).

Example of the Calculation of Oscillator Strengths:

Although the Coulomb approximation has been used extensively by many authors for the calculation of oscillator strengths, the following example is included in order to clarify the above discussion:

NI line, λ = 4151.46 Å

1. Look up the term values listed in (7) and write down a complete specification of the angular momenta

of the two levels involved in the transition:

$$2s^2 2p^2(^3P)3s(^4P_{5/2}) \rightarrow 2s^2 2p^2(^3P)4p(^4S^o_{3/2})$$

The usual selection rules are clearly obeyed by the transition ((8), pp 16 - 18).

2. Adjust the term values to refer to the ground state of the next highest stage of ionization, and reduce these to atomic units by dividing each by the factor 109679, i.e.

$\ell = 0$	$\ell = 1$
33848	9767
.3086	.0891

3. Denoting the orbital angular momenta of the two <u>electronic</u> levels involved by ℓ-1 and ℓ, determine the quantum numbers

$$n^*_{\ell-1} = \frac{C}{\sqrt{\text{reduced energy of lower level}}} = \frac{1}{\sqrt{.3086}} = 1.800$$

$$n^*_{\ell} = \frac{C}{\sqrt{\text{reduced energy of upper level}}} = \frac{1}{\sqrt{.0891}} = 3.350$$

where C = excess charge on nucleus after the active electron has been removed.

4. Look up the factors $\mathcal{F}(n^*_\ell , \ell)$ and $\mathcal{J}(n^*_{\ell-1}, n^*_\ell , \ell)$ in the tables of Bates and Damgaard (6), interpolating where necessary.

$$\mathcal{F}(3.350, 1) = 9.278$$

$$\mathcal{J}(1.800, 3.350, 1) = -.042$$

5. $\sigma = \frac{1}{C}\mathcal{F}\mathcal{J} = -.3897$ $\quad \therefore \sigma^2 = .1518$

6. Determine the Racah coefficients, and hence S(L) and S(M)

$J = 5/2$, $J' = 3/2$, $L = 1$, $L' = 0$, $S = \frac{3}{2}$

$\ell' = 0$, $\ell'' = 1$, $\ell_> = 1$, $L_1 = 1$

$W(LJL'J'; S1) = W(1\ 5/2\ 0\ 3/2\ ;\ 3/2\ \ 1) = .28868$

$W(\ell'L\ell''L'; L_1\ 1) = W(0\ 1\ 1\ 0\ ;\ 1\ 1) = .33333$

$\therefore$ $S(L) = .5000$ $\quad S(M) = 4$

[To check: identical values for S(L) and S(M) are found in (5), pp 56 - 64].

7. $S = S(M)S(L)\sigma^2 = .3036$

Statistical weight of lower level = $2J + 1 = 6$

$$\therefore \quad f = \frac{303.75\ S}{g_1 \lambda} = .0037$$

[cf. (1) : .00301 ; (7): .0023]

It is interesting that the older term value tabulations in (8) lead to a value of f in better agreement with the literature, viz. .00295.

Chapter 2 : Atomic Processes in the Plasma

It is pointed out in the Introduction that before line intensity ratios can be calculated, the type of thermodynamic situation that prevails in the plasma must be ascertained. When complete thermodynamic equilibrium exists, the ratio of the intensities of any given pair of lines belonging to successive ionization stages of the same element is a function of electron density and temperature alone. Where complete thermodynamic equilibrium does not prevail (as is the case with most laboratory plasmas), atomic processes need to be considered carefully.

Let S^z represent an atomic species, charge z. For the reversible reaction denoted by

$$S^z + e \rightleftarrows S^{z-1}$$

the following competing processes have to be taken into account:

(a) Three-body recombination, state p to state q

$$S^z(p) + e + e \rightarrow S^{z-1}(q) + e$$

(b) Collisional ionization (inverse of (a))

$$S^{z-1}(q) + e \rightarrow S^z(p) + e + e$$

(c) Radiative recombination

$$S^z(p) + e \rightarrow S^{z-1}(q) + h\nu$$

(d) Photo-ionization (inverse of (c))

$$S^{Z-1}(q) + h\nu \rightarrow S^{Z}(p) + e$$

(e) Collisional de-excitation

$$S^{Z-1}(p) + e \rightarrow S^{Z-1}(q) + e$$

(f) Collisional excitation (inverse of (e))

$$S^{Z-1}(q) + e \rightarrow S^{Z-1}(p) + e$$

(g) Spontaneous and stimulated emission

$$S^{Z-1}(p) \rightarrow S^{Z-1}(q) + h\nu$$

(h) Photo-excitation (inverse of (g))

$$S^{Z-1}(q) + h\nu \rightarrow S^{Z-1}(p)$$

(i) Auto-ionization

$$S_{*}^{Z-1}(p) \rightarrow S^{Z}(q) + e$$

The excitation of an electron other than the most loosely bound one or the simultaneous excitation of two electrons can result in a series of discrete states, some of which have energies greater than that required for normal ionization. Thus discrete lines for photon absorption could be observed in the midst of a continuous photo-ionization spectrum. A radiationless transition can now occur, giving rise to an ion ($S^{Z}(q)$) and free electron which have the same energy as the original ion. (Marr (9) p 168, Cooper (10) p 39)

(j) Di-electronic recombination (inverse of (i))

$$S^z(q) + e \rightarrow S_{**}^{z-1}(p) \rightarrow S^{z-1}(n) + h\nu$$

A reversible, radiationless transition occurs between an ion S^z in state q and an electron giving rise to a doubly excited bound level of S_{**}^{z-1} , followed subsequently by a radiative transition to a singly-excited state n of S^{z-1} below the ionization limit. It will be noticed that neither this process nor its inverse can occur in the case of hydrogenic systems since S^{z-1} must have at least two electrons. ((10), p 57).

Processes (i) and (j) are less important than the rest and are not further taken into account until the next chapter.

In connection with the ionization processes listed above, it should be noted that in a plasma the formation of an ion pair occurs for energies which are lower than the ionization energy of the isolated atom or ion. This is as a result of the fact that charges of one sign tend to have on the average an excess of charge of the opposite sign in their immediate neighbourhood. In (1) (pp 137 - 140) the Debye theory of Coulomb interactions in plasmas is discussed, and it is shown that the reduction of the ionization energy for a species of charge z-1 is given by

$$\Delta E_{\infty}^{z-1} = \frac{ze^2}{4\pi\varepsilon_o \rho_D} \qquad (2.1)$$

where E_{∞}^{z-1} = ionization energy

ρ_D = Debye length

$$= \left[\frac{\varepsilon_o kT}{e^2(N_e + \sum z^2 N_a^z)}\right]^{\frac{1}{2}} \qquad (2.2)$$

N_a^z = total no. of atoms per cm^3 with charge z.

In all cases dealt with in this thesis, this correction turns out to be a small fraction of an electron volt and is thus ignored. For example, in the case of NII , when

$$(N_e + \sum z^2 N_a^z) = 3.1 \times 10^{15}/cm^3$$

ΔE_{∞} increases from .007 eV at kT = 10 eV to .02 eV at kT = 1 eV whereas E_{∞} = 29.593 eV.

Processes resulting from atom-atom, atom-ion and ion-ion collisions are not included in this discussion, since the relevant rates are much smaller than those for electron-atom and electron-ion collisions in plasmas where the degree of ionization is appreciable ((10) p 42, (1) p 130). It is clear that processes (a), (b), (c), (e) and (f) depend upon the electron density and energies (characterized by electron temperature T_e). Via

collisional processes (mainly electron-electron, since momentum-transfer cross sections are small for particles of very different masses), the free electrons quickly attain statistical equilibrium provided three conditions are fulfilled (Wilson (11)).

These are

$$t_{ee} << t_{rad} , t_{en} , t_{part}$$

where t_{ee} is the electron-electron relaxation time, t_{rad} is the energy decay time for bremsstrahlung, t_{en} is the energy heating time and t_{part} is the particle containment time. Wilson shows that the first criterion is completely satisfied at all feasible temperatures, in laboratory plasmas. Spitzer (12) gives the following expression for the electron-electron relaxation (equilibrization) time:

$$t_{ee} = \frac{0.266\ T_e^{3/2}}{N_e\ \ell n\Lambda} \qquad (2.3)$$

where T_e is in ^{o}K and $\ell n\Lambda$ is a slowly varying function of electron density N_e and electron temperature T_e, usually of the order of 10 ((12) p 28, table 5.1). Thus in the case of a fully ionized Hydrogen plasma of electron density 10^{12} per cm^3, t_{ee} equals 2.82×10^{-8} sec. at 10^4 ^{o}K.

Under the above conditions, the velocity distribution of free electrons is Maxwellian, i.e.

$$dN_e(v) = 4\pi N_e \left(\frac{m}{2\pi\ kT_e}\right)^{3/2} \exp\left(\frac{-mv^2}{2kT_e}\right) v^2 dv \qquad (2.4)$$

where dN_e is the number of electrons per cm^3 with speeds between v and v + dv, and T_e , the parameter which characterizes each particular Maxwell distribution, is by definition the electron temperature.

For complete thermodynamic equilibrium, each possible process must occur at the same rate as its inverse (this is the "principle of detailed balance"). If one type of process is unbalanced, the plasma may nevertheless be in a state quite close to complete equilibrium. It is mentioned in the first chapter that photo-ionization, photo-excitation to higher-lying levels and stimulated emission occur at a negligible rate in most laboratory plasmas; spontaneous emission is thus unbalanced. If, however, the electron density and temperature are high enough collisional processes will occur at a far greater rate than radiative decay; and if these collisional processes nearly balance among themselves, the plasma will be in a state close to the thermodynamic equilibrium. One then speaks of local

thermal (or thermodynamic) equilibrium (LTE). In this case, population densities will be given by the Boltzmann and Saha equations to a high degree of accuracy (though not of course 100%):

$$\frac{N_n^{z-1}}{N_m^{z-1}} = \frac{g_n^{z-1}\ \exp(-E_n/kT_e)}{g_m^{z-1}\ \exp(-E_m/kT_e)} \qquad \text{(Boltzmann)} \qquad (2.5)$$

$$\frac{N_e N_1^z}{N_n^{z-1}} = \frac{2g_1^z}{g_n^{z-1}} \left(\frac{mkT}{2\pi\hbar^2}\right)^{3/2} \exp\ (-E_n'/kT_e) \qquad \text{(Saha)} \qquad (2.6)$$

In the Boltzmann equation, energies are expressed with respect to the ground state, whereas in the case of the Saha equation E_n' is the (positive) binding energy of state n, charge z-1, with respect to the ground state of the next ionization stage.

$$g = 2J + 1$$

$$\text{or} = 2n^2 \text{ (for hydrogenic levels)}$$

The temperature which describes the LTE is that of the electrons, since they dominate the reaction rates. The ions usually do not attain a Maxwellian velocity distribution within the lifetime of a laboratory plasma

and so one avoids assigning an ion temperature. For LTE to be a good approximation, fairly stringent conditions apply to the electron density and electron temperature of the plasma. In the case where the electron density is far too low at a given temperature for LTE to be valid, the corona model (so called since this type of situation prevails in the solar corona) leads to an equation of state which is approximately valid (Woolley and Allen (13)):

The three-body recombination rate is proportional to the square of the electron density, whereas the radiative recombination rate is proportional to the electron density alone, at a given temperature. Thus for low electron densities, the latter process dominates the recombination rates. One must therefore consider the approximate balance between collisional ionization (coefficient S) and radiative recombination (coefficient α). Let N_a^{z-1} and N_a^z be the total number of ions in two subsequent stages of ionization of a particular species. In the corona state, fractional ionization is determined by

$$\begin{aligned} S N_a^{z-1} N_e &= \alpha N_a^z N_e \\ \therefore \quad \frac{N_a^z}{N_a^{z-1}} &= \frac{S}{\alpha} \end{aligned} \tag{2.7}$$

which is independent of electron density. The evaluation of the rate coefficients S and α is considered in the next chapter.

In the régime between the thermal and coronal domains, the situation is much more complicated. In this connexion it is important to notice that collisional cross-sections increase with increasing principal quantum number, while radiative decay probabilities decrease (i.e. radiative lifetimes increase) ((1) p 130). Quantitatively, in the case of hydrogenic atoms, Bethe and Salpeter ((14), p 269) give the following expression for the reciprocal mean radiative lifetime R_n^{z-1} :

$$R_n^{z-1} = \sum_{n'<n} A_{n'n}^{z-1} \simeq 1.6 \times 10^{10} \frac{z^4}{n^{4.5}} \text{ sec}^{-1} \qquad (2.8)$$

where they have averaged over the initial ℓ-values according to their statistical weights.

Also, for most levels, cross-sections for collisional excitation are much larger than for de-excitation ((1) p 146). The conditions for LTE are thus especially stringent for lower-lying levels. Where the electron density at a particular temperature is too low for LTE to exist, another type of near-equilbrium state may

prevail, in which excitation and ionization from the ground state still occur by electron impacts, but radiative decay is the dominant mode of de-excitation between the lower-lying levels. However, the relative populations of the higher levels are usually still controlled by collisional processes, and there is coupling between the two groups of levels by collisionally induced transitions in both directions.

Thus, according to this model, the thermal equilibrium in the continuum extends down to the upper bound levels of the ion due to the high collisional transition rate between the continuum and upper levels, imposed by the free electrons. One may therefore postulate some level in the ion, the "thermal limit", above which the distribution is approximately thermal and below which it is approximately coronal. The Saha equation is applicable to these upper levels, and enables one to link their populations to the ground state population of the next (higher) ionization stage.

The resonance lines result from transitions from low-lying levels (i.e. below the thermal limit) to the ground state and contain far more energy than that radiated in the rest of the radiative transitions (cf. equation 2.8). For any possibility of approaching thermal equilibrium, these

lines, in contrast to the rest, must therefore be fairly strongly re-absorbed by the plasma and are not suitable for spectroscopic study (see also (1), Chapter 7).

Wilson (11) discusses work published on the semi-coronal distribution, and gives an expression for the domain of validity of the LTE approximation:

$$N_e \geq 6 \times 10^{13} (E_\infty)^3 (kT_e)^{1/2} \text{ cm}^{-3} \qquad (2.9)$$

(Here energies are expressed in eV.) For N_e far below this value at a particular temperature, the thermal limit is very close to the ionization limit and the coronal situation prevails. As N_e increases, the thermal limit drops until, at a sufficiently high density, it reaches the ground level and all levels have a thermal population i.e. the Boltzmann and Saha equations are generally valid. The derivation of an exact expression for the thermal limit is considered in the next chapter.

Formulae for the relative line intensities of subsequent ionization stages of the same element, valid under LTE and semi-coronal conditions, are derived below. Thus, if it could be established which of these models, or combination of models, describes a certain plasma, the electron temperature may be determined by measuring the intensities

of suitable spectral lines. The determination of the absolute intensity of a spectral line calls for very careful and accurate measurement, but by choosing pairs of lines and measuring their relative intensity one can eliminate some of the problems.

Line intensity ratios, LTE case:

Consider two subsequent ionization stages, z-1 and z, of the same element and let the two spectral lines of interest result from the following transitions:

z : Upper level m to lower level p, wavelength λ'

z-1 : Upper level n to lower level q, wavelength λ.

When no other superscript is used, primed quantities refer to the line from the higher ionization stage.

Boltzmann Equation:

$$\frac{N_m^z}{N_1^z} = \frac{g_m^z}{g_1^z} \exp(-E'/kT)$$

where $E' = E_m^z - E_1^z$ (excitation energy of higher level, higher ionization stage).

Saha Equation:

$$\frac{N_e N_1^Z}{N_n^{Z-1}} = \frac{2g_1^Z}{g_n^{Z-1}} \left(\frac{mkT}{2\pi\hbar^2} \right)^{3/2} \exp\left(- \frac{E_\infty^{Z-1} - E_n^{Z-1} + E_1^{Z-1}}{kT} \right)$$

Substituting from above, and putting $E_n^{Z-1} - E_1^{Z-1} = E$ (excitation energy of higher level, lower ionization stage) we obtain:

$$\frac{N_e N_m^Z}{N_n^{Z-1}} = \frac{2g_m^Z}{g_n^{Z-1}} \left(\frac{mkT}{2\pi\hbar^2} \right)^{3/2} \exp\left(- \frac{E' + E_\infty - E}{kT} \right)$$

Let I' be the intensity for the transition $N_m^Z \rightarrow N_p^Z$

I " " " " " " $N_n^{Z-1} \rightarrow N_q^{Z-1}$

Then, $I' = N_m^Z \; A'_{pm} \; h\nu'_{pm}$

$$= N_m^Z \left(\frac{2r_o \; \omega'^2_{pm}}{c} \right) \; h\nu'_{pm} \; \frac{g_p^Z}{g_m^Z} \; f'_{mp}$$

Similarly, $I = N_n^{Z-1} \; A_{qn} \; h\nu_{qn}$

$$= N_n^{Z-1} \left(\frac{2r_o \; \omega_{qn}^2}{c} \right) h\nu_{qn} \; \frac{g_q^{Z-1}}{g_n^{Z-1}} \; f_{nq}$$

(equations 1.1, 1.2)

$$\therefore \quad \frac{I'}{I} = \frac{N_m^Z \; \nu'^3 \; g_p^Z \; g_n^{Z-1} \; f'_{mp}}{N_n^{Z-1} \; \nu^3 g_q^{Z-1} \; g_m^Z \; f_{nq}}$$

Hence, substituting for $\frac{N_m^z}{N_n^{z-1}}$ from above,

$$\frac{I'}{I} = 2N_e^{-1} \left(\frac{mkT}{2\pi\hbar^2} \right)^{3/2} \frac{f'_{mp} \lambda^3 g'_p}{f_{nq} \lambda'^3 g_q} \exp\left(- \frac{E' + E_\infty - E}{kT} \right)$$

Introduce the Bohr radius a_o and ionization energy of Hydrogen, E_H :

$$a_o = \frac{4\pi \hbar^2 \varepsilon_o}{m e^2} \quad ; \quad E_H = \frac{m e^4}{32 \varepsilon_o^2 \hbar^2 \pi^2}$$

(MKS units)

$$\therefore \quad (4\pi^{3/2} a_o^3 E_H^{3/2})^{-1} = 2\left(\frac{m}{2\pi \hbar^2} \right)^{3/2}$$

Hence, substituting in the equation for $I'/_I$, we obtain

$$\frac{I'}{I} = \frac{f'g'\lambda^3}{f g \lambda'^3} (4\pi^{3/2} a_o^3 N_e)^{-1} \left(\frac{kT}{E_H} \right)^{3/2} \exp\left(- \frac{E' + E_\infty - E}{kT} \right)$$

(2.10)

in agreement with the relation stated without proof on p 272 of (1). In (2.10), g' and g are the statistical weights of the lower levels involved in the transitions, while E' and E are the (positive) excitation energies of the upper levels, referred to the ground states.

Line intensity ratios, semi-corona case:

Consider three subsequent ionization stages, z-1, z and z+1 of the same element (unprimed, primed and doubly primed respectively).

Let I' be the intensity for the transition $N_m^z \rightarrow N_p^z$

I " " " " " " $N_n^{z-1} \rightarrow N_q^{z-1}$

As before, $I' = N_m^z \left(\frac{2r_o \omega'^2_{pm}}{c} \right) h \nu'_{pm} \frac{g_p^z}{g_m^z} f_{mp}^z$

$$I = N_n^{z-1} \left(\frac{2r_o \omega^2_{qn}}{c} \right) h \nu_{qn} \frac{g_q^{z-1}}{g_n^{z-1}} f_{nq}^{z-1}$$

Assume that the upper level involved in each transition is in Boltzmann-Saha equilibrium with the ground state of the following ionization stage (i.e. that m and n are above their respective thermal limits). Then, from the Saha equation,

$$N_n^{z-1} = \frac{N_e N_1^z g_n^{z-1}}{2g_1^z} \left(\frac{2\pi \hbar^2}{mkT} \right)^{3/2} \exp \left(\frac{E_\infty - E_n^{z-1} + E_1^{z-1}}{kT} \right)$$

Similarly,

$$N_m^z = \frac{N_e N_1^{z+1} g_m^z}{2g_1^{z+1}} \left(\frac{2\pi \hbar^2}{mkT} \right)^{3/2} \exp \left(\frac{E'_\infty - E_m^z + E_1^z}{kT} \right)$$

A note on the Debye length:

Equation (2.2) is derived on the assumption that the ions have a Maxwellian distribution of speeds, at the same temperature as the electrons. In our case it would be more correct to assume a stationary ion background; the Debye length is then estimated by:

$$\rho_D = \left[\frac{\varepsilon_o \, kT}{e^2 \, N_e} \right]^{\frac{1}{2}} \qquad (2.12)$$

Equations (2.1) and (2.12) are used in the next chapter to give an indication of the highest bound level in a NII ion under laboratory and solar coronal conditions.

Chapter 3 : Mathematical Treatment of Rate Coefficients

§1 : Method of denoting energy levels: In the Boltzmann and Saha equations, the subscript n is used to distinguish between ionic energy levels (equations (2.5) and (2.6)). In the case of hydrogenic ions, where the electron states with the same principle quantum number are degenerate, a convenient way to indicate any level would thus be by the principle quantum number of the single bound electron. In the case of non-hydrogenic ions, the subscript n would no longer be a quantum number in the true sense, but merely a way of "counting" the levels from the ground state upward. The following derivation of the thermal limit applies primarily to hydrogenic ions; a method of employing the result in the case of non-hydrogenic ions is considered further on.

§2 : Derivation of the thermal limit for hydrogenic ions:

As stated in Chapter 2, the average radiative decay rate of a state with principal quantum number n is given by:

$$R_n^{Z-1} = \sum_{n'<n} A_{n'n}^{Z-1} \approx 1.6 \times 10^{10} \frac{Z^4}{n^{4.5}} \text{ sec}^{-1} \qquad (3.1)$$

According to Griem (1) (p 147), the collisional transition rate per atom or ion in state n to state n' is estimated by

$$C_{n'n}^{z-1} \simeq \frac{9 \times 10^{-8}}{z^3} f_{n'n} \; N_e \left(\frac{n'^3}{2}\right)\left(\frac{z^2 E_H}{kT_e}\right)^{\frac{1}{2}} \exp\left(-\frac{2z^2 E_H}{n'^3 kT_e}\right) \tag{3.2}$$

Let the principal quantum number n_t be chosen in such a way that for the corresponding level (the thermal limit), radiative decay is as likely as excitation into higher excited levels.

Since $\sum_{n'>n} f_{n'n} = 0.5\, n$ ((1) p160),

$$\sum_{n>n_t} C_{nn_t}^{z-1} \simeq \frac{9}{4} \times 10^{-8} \frac{n_t^4}{z^3} \; N_e \left(\frac{z^2 E_H}{kT_e}\right)^{\frac{1}{2}} \exp\left(-\frac{2z^2 E_H}{n_t^3 \, kT_e}\right) \tag{3.3}$$

With $R_n^{z-1} = \sum_{n>n_t} C_{nn_t}^{z-1}$, we find:

$$n_t \simeq 126 \; z^{14/17} \; N_e^{-2/17} \left(\frac{kT_e}{z^2 E_H}\right)^{1/17} \exp\left(\frac{4z^2 E_H}{17 \, n_t^3 \, kT_e}\right) \tag{3.4}$$

This definition of the thermal limit is by no means the only valid one. For example, a different n_t would be obtained by putting

$$R_n^{z-1} = \sum_{n>n_t} C_{nn_t}^{z-1} + C_{fn_t}^{z-1}$$

where $C_{fn_t}^{z-1}$ denotes the collisional ionization rate per ion in state n_t. This would also give a good indication of the lower limit of the collision-dominated régime. Wilson (11) adopts a third approach. (Note that in equation 6, (11), N_e^{-1} should be read for N_e).

§3 : The thermal limit for non-hydrogenic ions:

In Chapter 1, the effective principal quantum number n^* of a level E_n^{z-1} (meaning of n as in §1) is defined as

$$n^* = \frac{z}{\sqrt{\frac{E_\infty^{z-1} - E_n^{z-1}}{E_H}}}$$

Thus,

$$E_n^{z-1} = E_\infty^{z-1} - \frac{z^2 E_H}{n^{*2}} \qquad (3.5)$$

This may be compared with the corresponding hydrogenic expression, where one merely has n in place of n^*.

In the case of highly excited levels, the outer electron moves in a potential due to charge z, i.e. we assume that the screening due to the other bound electrons

is completely effective (the Coulomb approximation). These highly excited levels are thus hydrogenic, and n^* may be identified with the hydrogenic principal quantum number. Thus, provided that $\frac{z^2 E_H}{n_t^2}$ is small compared with E_∞, the expression for the thermal limit in §2 above is applicable, and in order to test whether the population of a given level is collision-dominated, one has merely to show that $n^* - n_t \gtrsim 0$.

§4 : Collisional-Radiative Coefficients:

When an electron is excited into a state for which the corresponding ionic level $n > n_t$, it is most likely to become a free electron before cascading down again (definition of thermal limit). Thus the effective ionization rate equals the sum of collisional rates for transitions from levels $n < n_t$ to $n \gtrsim n_t$ and collisional ionization rates from levels $n < n_t$. The effective recombination rate may be expressed as the sum of collisional and radiative rates from levels $n > n_t$ into levels $n \lesssim n_t$ and radiative recombination rates into levels $n \lesssim n_t$. Let $R_{cn"n}$ represent the rate at which collisional-induced transitions between n and n" occur and $R_{rnn"}$ the rate of spontaneous (radiative) transitions from n" to n. Denote the rates for collisional ionization from level n,

three-body recombination into level n and radiative recombination into level n by R_{cfn} , R_{cnf} and R_{rnf} respectively. Then in equilibrium, one has:

$$\sum_{n<n_t} R_{cfn} + \sum_{n''\geq n_t} \sum_{n<n_t} R_{cn''n} = \sum_{n\leq n_t} (R_{cnf} + R_{rnf}) + \sum_{n''>n_t} \sum_{n\leq n_t} (R_{cnn''} + R_{rnn''}) \tag{3.6}$$

Representing the summations on the left hand side of equation (3.6) by R_c , and the sum of the collisional terms and radiative terms on the right by R_c' and R_r respectively, the effective depopulation rate of the ground state becomes

$$\left.\frac{dN_1^{Z-1}}{dt}\right)_{\text{depopulation}} = -R_c \equiv -S_{cr} N_e N_a^{Z-1} \tag{3.7}$$

while the rate at which the ground state is populated is given by

$$\left.\frac{dN_1^{Z-1}}{dt}\right)_{\text{population}} = R_c' + R_r \equiv \alpha_{cr} N_e N_a^{Z} \tag{3.8}$$

In equilibrium, (3.7) and (3.8) must balance, i.e.

$$\frac{N_a^z}{N_a^{z-1}} = \frac{S_{cr}}{\alpha_{cr}} \qquad (3.9)$$

where S_{cr} and α_{cr} may be called the collisional-radiative ionization and recombination coefficients, respectively. In the limiting low-density (corona) case, where radiative de-excitation predominates over collisional de-excitation at all levels (i.e. the thermal limit merges with the continuum), S_{cr} and α_{cr} may be replaced by S and α (equation (2.7)).

It should be noted that the number of bound levels considered in equation (3.6) remains finite owing to the reduction of the ionization potential in a plasma. Where other processes such as auto-ionization and di-electronic recombination play a part, equation (3.9) should be replaced by

$$\frac{N_a^z}{N_a^{z-1}} = \frac{S_{tot}}{\alpha_{tot}} \qquad (3.10)$$

where $S_{tot} = S_{cr} + q_{auto}$

$\alpha_{tot} = \alpha_{cr} + \alpha_d$

Now the evaluation of these coefficients for a given

electron density and temperature presents great difficulties: the rate coefficient for each competing process is a complicated function of such parameters as temperature, density, ionization potential, ionic charge, initial and final quantum numbers. These functional forms are seldom well known over a wide range of conditions and generally present problems of extrapolation. Furthermore, in order to simplify the mathematical treatment, certain assumptions are introduced which, though perhaps reasonable under certain conditions, lead to fairly large inaccuracies in other cases. Significant disagreement is quite often found between formulae presented by different authors. Another difficulty is the rather misleading term "low density plasma": the density range is seldom specified although conclusions drawn for certain "low density" conditions are invalid for others.

In the rest of this chapter, some recent papers on the subject are discussed. It should be borne in mind that in our case the collisional-radiative coefficients necessary for the determination of line intensity ratios by means of equation (2.11), are required to be valid under the following conditions:

$$10^{15} < N_e < 10^{16} \text{ cm}^{-3}$$

$$1 < kT_e < 10 \text{ eV}$$

These criteria are justified in a later chapter.

In Wilson's paper (11) we find the following criteria for the thermal, coronal and semi-coronal domains:

Thermal Domain:

$$\log_{10} N_e \geq 13.7782 + 3 \log_{10} E_\infty + \tfrac{1}{2} \log_{10} kT_e \qquad (3.11)$$

Coronal Domain:

$$\log_{10} N_e \leq 10.1761 - \tfrac{1}{2} \log_{10} E_\infty + 4 \log_{10} kT_e \qquad (3.12)$$

Semi-Coronal Domain:

$$\log_{10} N_e \leq 11 + \tfrac{3}{2} \log_{10} E_\infty + 2 \log_{10} kT_e \qquad (3.13)$$

The fact that three independent authors are in reasonable agreement on equation (3.11) (McWhirter (15)) provides fair confidence in the selection of a lower limit to the thermal domain. The above three relations are graphed (fig.3.1) for the energy interval 1 eV to 100 eV for both NII and NIII; the curves suggest that since the domain we are considering lies on the periphery of the semi-coronal régime, equation (2.11) with appropriate collisional-radiative coefficients would give more realistic intensity

Fig. 3.1

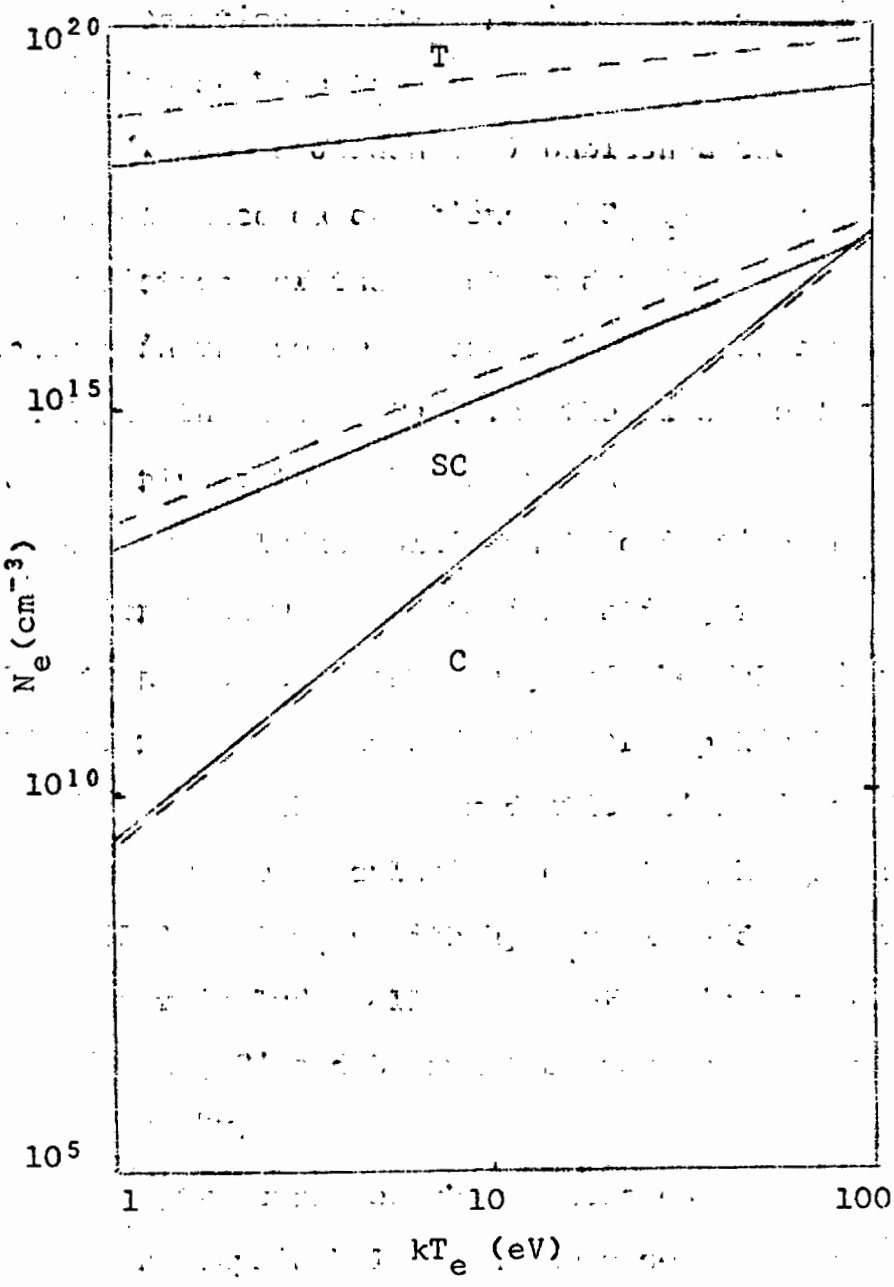

Graph of relations (3.11) - (3.13) (p 36) for NII and NIII (dotted line) ions. The following abbreviations are used: T : thermal domain; SC : semi-coronal domain; C : coronal domain.

incident electron by the Coulomb field of the nucleus. According to (19), Seaton's approximation is a good one for many cases, although there are a number of specific instances where it overestimates the rate coefficient by a factor of two or more.

The collisional ionization rate via bound levels was derived by Wilson in two later papers on the assumption that excitation to all levels above n_t is equivalent to ionization and that the levels above n_t are hydrogenic:

$$S(X^{+m}) = 4.8\times10^{-5}\ z^{-2} T_e^{-1/2}\ e^{-I_i/kT_e}\ n_t^{-2}\ e^{-\chi_t/kT_e} \qquad (3.15)$$

where χ_t, the ionization energy of level n_t, is given by

$$\chi_t^7 = 6 \times 10^{-28} \frac{I_i}{kT_e} N_e^2 \qquad (3.16)$$

and the effective charge z equals m+1. These two equations are employed in (16).

Unfortunately, the more recent papers of Wilson(1964, 1967) could not be consulted as these were published in reports not generally available. Thus it is not clear how the above two equations were derived. In (11), however, we find the same expression for χ_t , except that the numerical factor is half as large (equation 7, (11)).

Now the latter equation was derived from Wilson's expression for the thermal limit, on the assumption that $E_\infty^{z-1} = z^2 E_H$, which is certainly not true in general.

Thus equation 7, (11) should read:

$$\chi_t^7 = 2.78 \times 10^{-28} \frac{z^2 E_H}{kT_e} N_e^2$$

However, since Jordan obtains n_t from equation (3.4), it seems more consistent to use a value of χ_t derived directly from the calculated value of the thermal limit, i.e.

$$\chi_t = \frac{z^2 E_H}{n_t^2} \qquad (3.17)$$

For order-of-magnitude calculations, these considerations are not particularly important.

Jordan has found that for electron densities and temperatures in the solar corona and chromosphere, the collisional ionization rate via bound levels is negligible compared with direct collisional ionization, and has apparently neglected the former in both sets of calculations. This conclusion is examined below:

For the ion NII at an electron temperature of 2 eV, we find that the rate coefficient for direct collisional ionization

$$q = 2.62 \times 10^{-15} \text{ cm}^3 \text{ sec}^{-1}$$

Allow the electron density to decrease from a typical laboratory value of 3×10^{15} cm^{-3} to a typical (solar) coronal value of 3×10^{10} cm^{-3}, while keeping the temperature constant. The Debye length then increases from 1.92×10^{-7} m to 6.07×10^{-5} m, and as a result the lowering of the ionization potential decreases from 1.50×10^{-7} eV to 4.74×10^{-5} eV. The effective quantum number of the highest bound level changes from about 60 to 1071, while n_t increases from roughly 3 to 10.7.

With χ_t given by (3.17) the collisional ionization rate via bound levels changes from 1.6×10^{-16} to 2.0×10^{-16} cm^3 sec^{-1}. The slow variation in S is probably due to the fact that as n_t increases, the number of bound levels also increases owing to the corresponding change in the Debye length. Thus it appears that although S is certainly smaller than q, neglecting it completely leads to less accurate results than would otherwise be obtained.

§6 : Auto-ionization:

Several simplifying assumptions are introduced in Jordan's evaluation of the auto-ionization rate, this process being most important in the case of atoms where there are a large number of electrons in the first inner shell compared with the number in the outer shell (e.g. NaI, MgI, CaI, KI, BI, CI). Cox and Tucker (19) neglect auto-ionization entirely in their calculations (H, He, C, N, O, Ne, Mg, Si and S) - in contradiction to Jordan as far as the elements Mg and C are concerned. However, since this process is relatively unimportant for the lighter elements, any inaccuracy in the assumed auto-ionization formulae for the element N should make little difference to the final result.

§7 : Radiative Recombination:

For temperatures less than $T_e = 6 \times 10^5$ °K, the radiative recombination rate of Elwert is used by Jordan

$$\alpha(X^{+m}) = 0.97 \times 10^{-12} I_m n_o g T_e^{-1/2} \text{ cm}^3 \text{ sec}^{-1} \quad (3.18)$$

where n_o is the ground state principal quantum number; $g = 3$ for lighter atoms and I_m is the ionization energy.

Assuming the levels above n_t to be hydrogenic, Wilson (1967) derived the following expression for the radiative recombination rate via bound levels (i.e. radiative decay rate from bound levels above the thermal limit):

$$\alpha_b \simeq 1.2 \times 10^{-6}\ z^4\ T_e^{-3/2}\ n_t^{-1}\ \exp(\chi_t/kT)\ \text{cm}^3\ \text{sec}^{-1} \qquad (3.19)$$

(z is the charge on the recombining ion). Jordan has apparently neglected the latter process in the second set of calculations.

Consider again the imaginary experiment in §5 above. While

$$\alpha = 7.665 \times 10^{-13},$$

the radiative decay rate changes from

$$\alpha_b = 3.71 \times 10^{-11} \quad \text{at the higher density}$$

to $$\alpha_b = 6.445 \times 10^{-13} \quad \text{at the lower density.}$$

Jordan finds that "in low ions, such as CII, OII, SiII, this process is comparable with the direct recombination rate" (i.e. under solar conditions).

Under laboratory conditions, it appears to be the dominant mode of radiative recombination.

§8 : Collisional de-excitation and 3-body recombination:

In (16), the recombination rate resulting from collisional de-excitation of levels above the thermal limit ($\alpha_{coll.b}$) and the three-body recombination from the continuum into levels below the thermal limit ($\alpha_{coll.c}$) were calculated using expressions given by Wilson (1967):

$$\alpha_{coll.b} = 2.0 \times 10^{-20} N_e z^{-2} T_e^{-2} \exp(\chi_t/kT) n_t^{-2} \text{ cm}^3 \text{ sec}^{-1} \quad (3.20)$$

$$\alpha_{coll.c} = 6 \times 10^{-21} N_e z^{-2} T_e^{-2} \text{ cm}^3 \text{ sec}^{-1} \quad (3.21)$$

"It was found that both processes can be neglected in solar conditions".

Let the density decrease at 2 eV as in §5 above. We find that $\alpha_{coll.b}$ changes from

$$\alpha_{coll.b} = 6.34 \times 10^{-14} \text{ to } 3.088 \times 10^{-21}$$

while the three-body rate varies from

$$\alpha_{coll.c} = 8.353 \times 10^{-15} \text{ to } 8.353 \times 10^{-20}$$

Thus although both coefficients are much larger under

our conditions, they still appear to be relatively unimportant.

§9 : Di-electronic recombination:

Simplified expressions for this rate coefficient have been developed by A. Burgess (20), (21) who first pointed out its importance. These expressions are valid to within 20 per cent under coronal conditions where $N_e < 10^9$ cm^{-3} ; at higher densities, however, there are no reliable formulae which can be applied. Burgess argues that since the highly excited states above n_t effectively become part of the continuum, these states should not be included in the summation in the di-electronic rate. He considers the ion CaII and suggests an effective reduction in the di-electronic rate at higher densities:

$$D = \sum_{n=4}^{n_t} \alpha_d(n) / \sum_{n=4}^{\infty} \alpha_d(n) \qquad (3.22)$$

where $\alpha_d(n) = \sum_{\ell} \alpha_d(i,j,n\ell)$, i being the initial state of the recombining ion. His values of D for different n_t are tabulated below:

n_t	D
200	0.91
100	0.62
60	0.43
20	0.15
10	0.06
8	0.04
6	0.02

In view of the lack of accurate calculations for each ion, Jordan used these CaII values for all ions, as very approximate reduction factors. Thus, in our case the effective rate

$$\alpha_d(\text{eff}) = D\alpha_d << \alpha_d \qquad (3.23)$$

since n_t is typically small compared with 200. In their general treatment of recombination in a low-density plasma, neither Jordan nor Cox and Tucker find it necessary to allow for this reduction. In their case, although di-electronic recombination is negligible at low energies (about 1 eV), it could become the dominant recombination mode by 10 eV; in our case, if Burgess is correct, it probably remains unimportant over the whole energy range of interest.

§10 : Conclusion:

The above discussion shows clearly that calculated values of S/α in the literature are not applicable under our conditions. It was therefore decided to use the H_β line profile to ascertain electron densities, measure relative line intensities for NIII and NII lines, and determine S/α by means of equation (2.11) by allowing the temperature to be a running variable in the range of 1 to 10 eV. Large variations in the value of S/α at all temperatures for the line ratios selected, would then presumably indicate that the semi-coronal model used to derive equation (2.11) is not applicable under the conditions studied. The results of such an experiment are tabulated in Chapter 5.

Chapter 4 : Experimental Method

§1 : Experimental arrangement:

Two separate investigations were carried out; the circuitry for the first of these is illustrated in fig. 4.1. Two 8.5 μf capacitors were charged in parallel to 16 KV through the 500 KΩ resistors as shown, by means of an H.T. supply. A trigger pulse from the thyratron then closed switches A and B, and the capacitors discharged in series in a circuit which included a theta pinch (copper coil wound around a cylindrical glass tube of length 60 cm and outer diameter 3.4 cm, containing the hydrogen and nitrogen mixture at a pressure of 100 millitorr).

In the second investigation, roughly the same arrangement was used. The bank consisted of pairs of capacitors charged in parallel and discharged in series. There were 7 of these pairs, of which 6 were used for the main discharge and 1 for the preheater discharge.† A larger theta pinch (length 74 cm, outer diameter 10 cm) was employed. A crowbar switch ensured that the discharge current started decaying exponentially after the first quarter period.

Details of the apparatus are summarized below:

---

†Because the preheater gave rise to impurities in the plasma, all 7 pairs were later used for the main discharge and only rf preheating was used.

Fig. 4.1

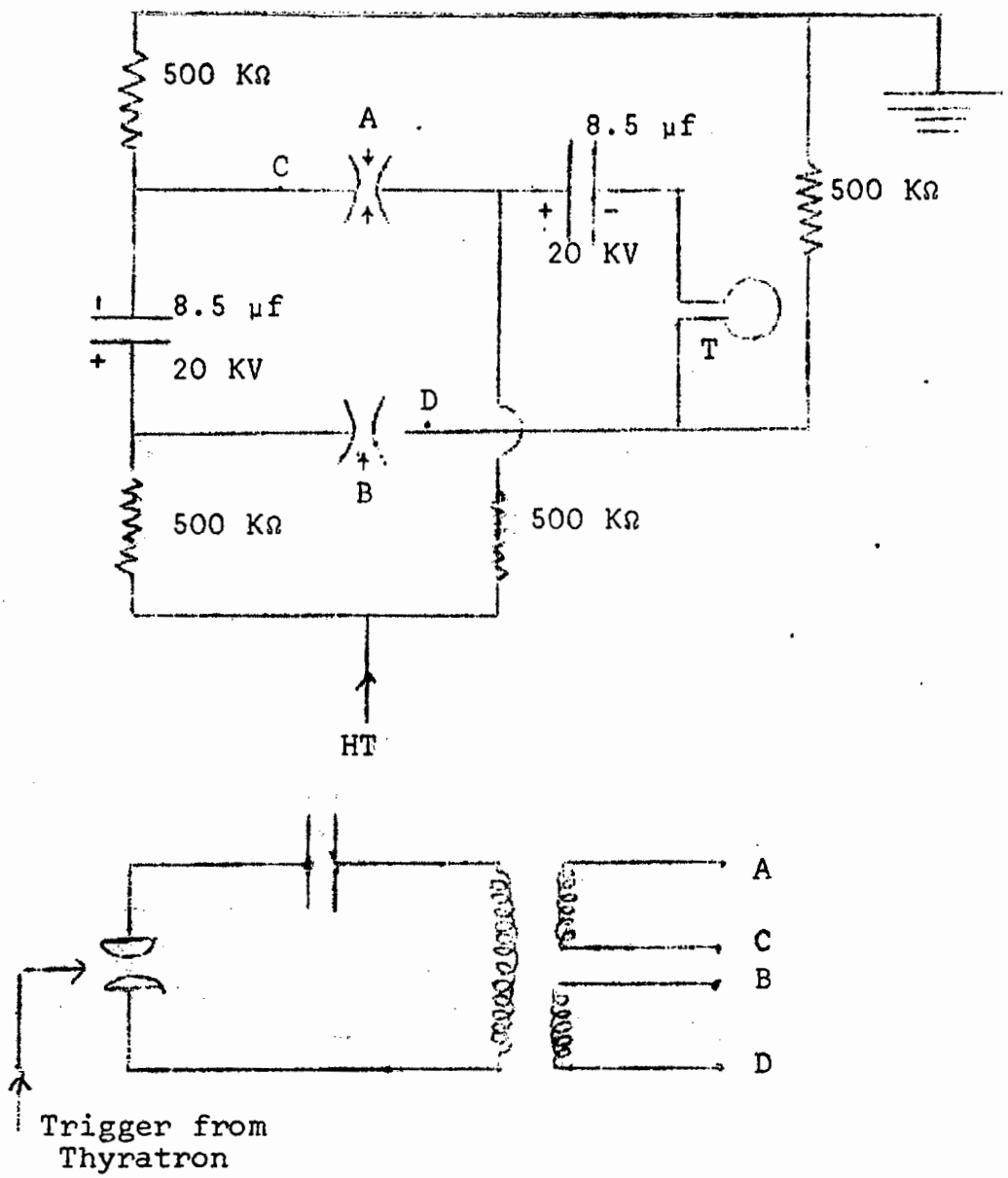

Circuitry for production of theta pinch plasma in T

	Expt.1	Expt.2
Bank Voltage (KV)	16	12
Bank Energy (KJ)	2.18	8.57
Peak Current (KA)	212	828
Total Inductance (nH)	263	68
Coil Inductance (nH)	12	31
Discharge Period (μ sec)	6.7	.9 (not crow-barred)
Preheater	rf	rf
Preheater Energy (KJ)	-	-
Crow-barred	No	Yes
Coil Length (cm)	9.5	32
Tube Length (cm)	60	74

Nitrogen gas constituted a small (5%) impurity in a fully ionized hydrogen plasma. The light intensity radiated at a particular wavelength was recorded by means of a photomultiplier connected to the exit slit of a Heath Scanning Monochromator with dispersion 20 Å/mm. The entrance and exit slits were usually set at 3 microns and 4 Å, respectively, for the first experiment; for the second experiment, an entrance slit setting of 7 microns was found to be more suitable.

The following NII and NIII lines were selected for study on the basis of

a) oscillator strength above 0.1

b) observed intensity

c) wavelength above 3800 Å and below 6200 Å (range determined by characteristics of photo-multiplier)

d) chosen line at least 4 Å away from nearest line in wavelength tables:

NII (λ in Å)	NIII (λ in Å)
3838.39	4003.64
3919.01	4097.31
3995.00	4103.37
4026.08	4195.70
4133.67	4200.02
4176.16	
4227.75	
4447.03	
4530.40	
4552.54	
4630.54	

§2 : Determination of electron density:

This was achieved by scanning the profile of H_β (4861.32 Å) from about 4840 Å to 4880 Å with entrance and exit slits of the monochromator set at a fixed value

(about 5 microns). The continuum (background) radiation was measured at 4880 Å and 4950 Å and the average subtracted from the height of the profile, in order to determine the full width at half maximum (the so-called "half-width").

W.L. Wiese (22) has plotted the half-width of H_β against electron density from detailed Stark-broadening calculations. The graph is valid for a temperature range of 5000 °K to 40,000 °K, the variation of half-width with temperature being negligible. According to the author, "the very good agreement between theory and experiment indicates that the resulting electron densities are accurate to about 7 per cent, provided that the experimental errors can be kept small".

In our case, the major source of error was the sketching of the outline of the profile through experimentally determined points, which could have led to an estimated 10 per cent error in electron density. However, this uncertainty in N_e was found to be negligible in comparison with the percentage variation in S/α (see Chapter 5).

This method of determining N_e is highly satisfactory, since Stark broadening is principally a density effect and

does not depend on either electron temperature or electron velocity distribution, i.e. it is essentially independent of the assumption of LTE. "Hence Stark broadening measurements will give reliable electron densities even in cases where the existence of LTE is doubtful, whereas some other methods would then become invalid" (22).

§ 3 : Determination of electron temperature:

Using formulae for recombination radiation and bremsstrahlung combined with the Saha equation, Griem ((1) p 279) calculates the ratio of total integrated line intensity to continuum intensity (in a 100 Å band centred at the line) as a function of temperature. The results are plotted for several HeI, HeII and Balmer lines. According to Griem, "deviations from LTE cause no great errors as long as electron densities are above 10^{14} cm^{-3} (in the case of H_β)".

By means of the monochromator, the line to continuum ratio could be fairly accurately determined. Since T_e enters in the exponential only, in equations (2.10) and (2.11), larger percentage errors could be tolerated than with N_e (in equation (2.11)). It was difficult to

determine the error, the main source of which was probably the theoretical curve.

§4 : Reproducibility of data:

The major limitation in these experiments was the reproducibility of the spectral lines observed. The reproducibility was found to be better for NII lines than for NIII lines. In the case of the larger crowbarred theta pinch, the reproducibility was found to be excellent.

Chapter 5 : Discussion of Results

§1 : Calculated f-values: For purposes of comparison, the values given by Griem (1) and Wiese, Smith and Glennon (7) are also tabulated below. Here n^* is the effective principal quantum number of the higher level involved in the transition.

Ion	Wavelength	n^*	This work	Griem	W.S.G.
NIII	4003.64	4.98	.677	.677	.674
NIII	4097.31	2.68	.484	.484	.486
NIII	4103.37	2.68	.241	.242	.244
NIII	4195.70	4.00	.948* (a)	.442	.442
NIII	4200.02	4.00	.852* (a)	.398	.398
NII	3838.39(e)	3.23	.114	.114	.116
NII	3919.01	3.00	.229	.229	.231
NII	3995.00	2.61	.613*	.613	.63
NII	4026.08	4.01	- (d)	-	.280
NII	4133.67	7.02	- (b)	.118*	.117
NII	4176.16	3.98	.74 (b)	.818*	.80
NII	4227.75(e)	3.28	.170	.171	.171
NII	4447.03	2.92	.59 (c)	.587*	.642
NII	4530.40	4.01	.903*	.909	.67
NII	4552.54	4.01	- (d)	-	.305
NII	4630.54	2.54	.240*	.239	.269

* : f-value used in calculations

(a) : all values quoted in (1) and (7) for this multiplet, are too small by a constant factor 2.14

(b) : extrapolation necessary far outside range of tables in (6)

(c) : minor extrapolation necessary

(d) : selection rule violated; hence not suitable for calculation by Coulomb approximation

(e) : p-s transition.

§2 : Density and Temperature Measurements:

From measurements of the half-width of H_β , the electron density in the small theta pinch was found to be close to 3×10^{15} cm^{-3}. This value did not vary appreciably over the whole time interval of interest (2 μsec to 18 μsec after the start of the discharge) and N_e was therefore taken to be a constant in the calculations. In the case of the small theta pinch, the discharge current was not crow-barred and the line to continuum ratio for H_β was found to be completely unreliable. This was probably due to plasma contamination.

The following values were obtained with the large (crow-barred) theta pinch:

Time (μsec)	$N_e(cm^{-3})$	kT_e (from H_β line to continuum)
2	8×10^{15}	4.5
4	8×10^{15}	3.6
6	1.3×10^{16}	3.0
8	1.1×10^{16}	2.6
10	9.5×10^{15}	2.4
12	8×10^{15}	2.0
14	7×10^{15}	1.6
16	6×10^{15}	1.4
18	4.5×10^{15}	1.1

§3 : Temperature predictions by LTE formula:

A large amount of data was obtained from computer calculations, for the lines selected. Only the important results can be briefly summarized here.

It was found that for times later than about 4 μsec after the current had been crow-barred, equation (2.10) predicted temperatures of the correct order of magnitude. These predicted temperatures were obtained from calculations of I'/I over the range $1 \leq kT_e \leq 10$ eV in steps of 1 eV and then over the range $1 \leq kT_e \leq 3$ eV in steps of .2 eV. The temperature that fitted the experimental observations the

closest, however, remained very nearly constant throughout the time interval, whereas line to continuum measurements for the large theta pinch indicate that by 18 μsec after the bank has started discharging, the electron temperature has dropped to about half of its value at 6 μsec.

Consider, for example, the line pairs 4003.64/4447.03, 4103.37/4630.54, 4200.02/3838.39. The following intensity ratios were measured with the large theta pinch:

Time (μsec)	$\frac{I'}{I}$ 4003.64 / 4447.03	$\frac{I'}{I}$ 4103.37 / 4026.08	$\frac{I'}{I}$ 4200.02 / 3838.39
2	0.45	4.02	2.93
4	0.61	1.83	4.03
6	0.39	0.98	1.38
8	0.27	0.78	1.11
10	0.17	0.61	1.25
12	0.07	0.51	1.66
14	0.02	0.54	1.83

The LTE programme, with a constant electron density of 10^{16} cm^{-3} , gave:

kT_e	I'/I 4003.64 / 4447.03	4103.37 / 4026.08	4200.02 / 3838.39
1.2	$.220 \times 10^{-6}$	$.297 \times 10^{-4}$	$.110 \times 10^{-5}$
1.4	$.203 \times 10^{-4}$	$.938 \times 10^{-3}$	$.853 \times 10^{-4}$
1.6	$.622 \times 10^{-3}$	$.128 \times 10^{-1}$	$.229 \times 10^{-2}$
1.8	$.909 \times 10^{-2}$	.100	$.301 \times 10^{-1}$
2.0	$.790 \times 10^{-1}$	.528	.241
2.2	.470	$.208 \times 10$	$.134 \times 10$
2.4	$.210 \times 10$	$.662 \times 10$	$.565 \times 10$
2.6	$.753 \times 10$	$.178 \times 10^2$	$.193 \times 10^2$
2.8	$.227 \times 10^2$	$.418 \times 10^2$	$.558 \times 10^2$
3.0	$.593 \times 10^2$	$.882 \times 10^2$	$.141 \times 10^3$

Predicted temperatures: (kT_e in eV).

Time (μsec)			
2	2.2	2.3	2.3
4	2.2	2.2	2.4
6	2.2	2.1	2.2
8	2.2	2.0	2.2
10	2.1	2.0	2.2
12	2.0	2.0	2.2
14	2.0	2.0	2.2

A value of kT_e between 2.0 and 2.2 eV is thus predicted over most of the time range.

Equation (2.10) is thus rather insensitive to changes in I'/I, and seems to provide a measure of the mean electron temperature rather than its behaviour against time.

Another important result is that the variation of the temperatures predicted by most of the line intensity ratios is not greater than about 0.4 eV at any time. It is interesting to note that pairs of lines with lower values of n^* provide consistently low temperature estimates, whereas the reverse is true for pairs with higher values of n^*, e.g.

Time (μsec)	4103.37 / 4630.54	4097.31 / 3995.00	4003.64 / 4530.40
2	1.7	1.8	2.7
4	1.6	1.7	2.7
6	1.6	1.7	2.6
8	1.6	1.6	2.5
10	1.6	1.6	2.4
12	1.5	1.6	2.3
14	1.5	1.5	2.2

The temperatures in the third column above should be more reliable; the lower n^*, the less accurate the assumption that the particular level is thermally populated (see n^* values in §1 above).

4 : Calculated values of S/α :

By means of equation (2.11) with measured I'/I values, the coefficient S/α was obtained for

$$1.0 \leqslant kT_e \leqslant 10$$

in steps of .5 eV, and times 2 to 18 μsec in steps of 2 μsec. At each time, variations of over 100 per cent about the mean were found for the line ratios selected, instead of the constant values expected at least one temperature (the value nearest the correct one).

This may perhaps be explained as follows. Typical values for the thermal limits of NII and NIII, respectively, under the conditions described in §2 above, are

$$n_t = 3 \text{ and } n_t = 4$$

(from equation (3.4))

In Chapter 2, equation (2.11) is derived on the assumption that the upper level involved in each transition lies above the themal limit for that particular ion. No attempt is made to predict the inaccuracies involved if n^* is less than n_t ; in general, however, it may be stated that calculated f-values as well as S/α values improve the closer n^* is to the ionization limit.

Thus, "best" values of S/α would be expected for the

NIII line 4003.64 Å, and the NII lines 4026.08, 4133.67, 4552.54 and 4530.40 Å. Unfortunately, the 4133.67 Å NII line was far less intense than the rest, and measurements were considered unreliable because of the comparatively large background intensity in the vicinity. "Worst" values would be expected for 4097.31/3995.00, 4103.37/4630.54 for example.

The following values were obtained with the large theta pinch. The temperatures given are those in the computer programme nearest the H_β line-to-continuum results in §2 above. An asterisk indicates an unreliable result, which is not included in the mean.

NIII/NII	Time (μsec)	kT_e(eV)	S/α	mean S/α
4003.64/4026.08	2	4.5	0.10	
4003.64/4530.40			0.20	0.12
4003.64/4552.54			0.07	
4097.31/3995.00			0.06*	
4103.37/4630.54			0.05*	
4003.64/4026.08	4	3.5	0.08	
4003.64/4530.40			0.13	0.09
4003.64/4552.54			0.06	
4097.31/3995.00			0.02*	
4103.37/4630.54			0.02*	
4003.64/4026.08	6	3.0	0.03	
4003.64/4530.40			0.05	0.04
4003.64/4552.54			0.03	
4097.31/3995.00			0.01*	
4103.37/4630.54			0.01*	
4003.64/4026.08	8	2.5	0.02	
4003.64/4530.40			0.03	0.023
4003.64/4552.54			0.02	
4097.31/3995.00			0.01*	
4103.37/4630.54			0.00*	
4003.64/4026.08	10	2.5	0.01	
4003.64/4530.40			0.02	0.017
4003.64/4552.54			0.02	
4097.31/3995.00			0.00*	
4103.37/4630.54			0.00*	
4003.64/4026.08	12	2.0	0.01	
4003.64/4530.40			0.01	0.010
4003.64/4552.54			0.01	
4097.31/3995.00			0.00*	
4103.37/4630.54			0.00*	
4003.64/4026.08	14	1.5	0.00	
4003.64/4530.40			0.00	0.00
4003.64/4552.54			0.00	
4097.31/3995.00			0.00	
4103.37/4630.54			0.00	

In (16), the second set of calculations (i.e. for a general "low density" plasma) gives:

$$S/\alpha = 2.1 \times 10^{-4} \text{ at } 3.4 \text{ eV}$$

$$\text{and} = 2.1 \times 10^{-3} \text{ at } 4.3 \text{ eV}.$$

The following are estimates of NIV/NIII from the Saha equation, where the partition functions are approximated by the statistical weights of the respective ground states:

kT_e(eV)	N_e(cm^{-3})	NIV/NIII
4.5		25.2
4.0	10^{16}(constant)	5.7
3.5		0.85
3.0		0.07
2.5		0.00
2.0		0.00

§5 : Conclusion:

The ratios of NIV/NIII obtained lie between the values predicted for LTE and near-coronal conditions (apart from the small discrepancy at lower temperatures, where the experimental values appear to be very slightly too high). When the density is kept nearly constant, the observed values approach the coronal at higher temperatures. This

is in agreement with fig. 3.1 and is indeed what one would expect: the mean free path of the free electrons increases with T_e at a constant density. Thus the rate coefficients for collisional processes should increase more slowly than in the LTE case, with the result that N_a^z/N_a^{z-1} should be smaller than the values obtained from the Saha equation. [The inequality in 2b of (11) appears to be a misprint] .

A disadvantage of our approach is that formulae derived for a time-independent homogeneous plasma are being applied to a transient one which cannot be expected to be completely homogeneous (although, however, no NI or NIV were observed under our conditions). Since electron densities were known to be below these required for LTE, the equilibrization times for the various processes were greater than in the LTE case. Thus a possible explanation of the observation that equation (2.10) gave temperatures that were too high at the end, is that the decrease in the NIII/NII ratio was slower than that expected under LTE conditions.

The role of the effective principal quantum number n^* in relation to the calculated value of the thermal limit n_t is seen to be very important. Where n^* is too close

to or less than n_t , values obtained for S/α must be expected to be too small (i.e. closer to coronal, at a given temperature) since the assumptions used in deriving (2.11) are no longer accurately satisfied. For lines resulting from transitions from levels near the ionization limit, the assumption that these levels are thermally populated would be better fulfilled with the result that improved values of S/α could be expected (below 3.5 eV however the values obtained seem to be of the correct order of magnitude). Unfortunately, our careful scanning of the Nitrogen spectrum indicated that the lines examined were the only satisfactory ones from an experimental point of view, in the optical wavelength region.

In view of the remarks above, our values of S/α must be regarded as tentative, until further work has been carried out to improve upon their accuracy or determine the probable errors involved. Because of the present lack of knowledge of the rate coefficients necessary for a theoretical determination of S/α it was hoped to obtain values that would enable accurate temperature determinations to be carried out from measured line intensity ratios.

However for an order of magnitude temperature estimate the present values could be considered reasonably satisfactory.

Bibliography

(1) H.R. Griem, "Plasma Spectroscopy", McGraw-Hill 1964

(2) H.N. Russell, Astrophys. J. (1936) 83, 129-139

(3) L. Goldberg, Astrophys. J. (1935) 82, 1-25

(4) L. Goldberg, Astrophys. J. (1936) 84, 11-13

(5) C.W. Allen, "Astrophysical Quantities", Athlone Press 1964

(6) D.R. Bates and A. Damgaard, Phil. Trans. Roy. Soc. London (1949) Ser A., 242, 101-122

(7) W.L. Wiese, M.W. Smith, B.M. Glennon, "Atomic Transition Probabilities" Vol I (Hydrogen through Neon), 1966, NSRDS-NBS 4- (National Bureau of Standards)

(8) R.F. Bacher and S. Goudsmit, "Atomic Energy States", McGraw-Hill 1932

(9) G.V. Marr, "Plasma Spectroscopy", Elsevier 1968

(10) J. Cooper, Reports on Progress in Physics (1966), 29 Part 1, 35-130

(11) R. Wilson, J. Quant. Spectrosc. Radiat. Transfer (1962) 2, 477-490

(12) L. Spitzer, "Physics of Fully Ionized Gases", Interscience 1962

(13) R. v.d. R. Woolley and C.W. Allen, M.N.R.A.S., (1948) 108, 292-305

(14) H.A. Bethe and E.E. Salpeter, "Quantum Mechanics of One- and Two-Electron Atoms", Academic Press 1957

(15) R.W.P. McWhirter, "Spectral Intensities". Ch 5 of "Plasma Diagnostic Techniques", edited by R.H. Huddlestone and S.L. Leonard, Academic Press 1965

(16) C. Jordan, M.N.R.A.S. (1969) 142, 501-521

(17) D.R. Bates, A.E. Kingston and R.W.P. McWhirter, Proc. Roy. Soc. A (1962) 267, 297-312

(18) M.J. Seaton, Planet. Space Sci.(1964) 12, 55-72

(19) D.P. Cox and W.H. Tucker, Astrophys. J. (1969) 157, 1157-1167

(20) A. Burgess, Astrophys. J. (1964) 139, 776-780

(21) A. Burgess, Astrophys. J. (1965) 141, 1588-1590

(22) W.L. Wiese, "Line Broadening", Ch 6 of "Plasma Diagnostic Techniques", op.cit. (15) above